Z mode waves as the source of Saturn narrowband radio emissions

Sheng-Yi Ye,[1] J. D. Menietti,[1] G. Fischer,[2] Z. Wang,[1] B. Cecconi,[3] D. A. Gurnett,[1] and W. S. Kurth[1]

Received 4 December 2009; revised 15 March 2010; accepted 21 April 2010; published 28 August 2010.

[1] We report 5 kHz narrowband Z mode emissions observed by the Cassini Radio and Plasma Waves Science (RPWS) instrument during high latitude perikrone passes. The narrowband emissions observed below the local electron cyclotron frequency (f_{ce}) are >20 dB more intense than the usual L-O mode narrowband emissions observed above local f_{ce}. Polarization measurements show that the narrowband emissions observed below f_{ce} are oppositely polarized to those above f_{ce}, which identifies the emissions below f_{ce} with Z mode. We propose that the L-O mode narrowband emissions observed at 5 kHz are mode converted from the Z mode waves at a density gradient or density irregularity. The Z mode to L-O mode conversion via scattering off of density irregularities can also account for the direction finding results of 5 kHz narrowband emissions which point to a source in the auroral zone. We also present the first magnetic field measurements of Saturn narrowband emissions validating their electromagnetic nature.

Citation: Ye, S.-Y., J. D. Menietti, G. Fischer, Z. Wang, B. Cecconi, D. A. Gurnett, and W. S. Kurth (2010), Z mode waves as the source of Saturn narrowband radio emissions, *J. Geophys. Res.*, *115*, A08228, doi:10.1029/2009JA015167.

1. Introduction

[2] Saturn narrowband emissions, first detected during the Voyager 1 flyby of Saturn [*Gurnett et al.*, 1981], are most prominent at 5 kHz. They typically occur periodically after an intensification of Saturn kilometric radiation (SKR) and last for several days [*Louarn et al.*, 2007; *Wang et al.*, 2010]. Higher frequency (from 10 to 70 kHz) but less intense narrowband emissions are referred to as 20 kHz narrowband emissions by *Wang et al.* [2010] and *Ye et al.* [2009]. Both the 5 kHz and 20 kHz narrowband emissions are found to be emitted in the left-hand ordinary (L-O) mode [*Ye et al.*, 2009]. Statistics on Cassini observation of Saturn narrowband radio emissions show that the 5 kHz narrowband emissions are detected at all latitudes covered by the spacecraft whereas the 20 kHz narrowband emissions are only observed at relatively high latitudes [*Wang et al.*, 2010]. Saturn narrowband emissions are modulated with a period around 10.8 hours, near the nominal rotational period of Saturn. It is shown that the rotational modulation of the 5 kHz narrowband emissions resembles that of SKR, which indicates a clock-like source [*Wang et al.*, 2010].

[3] Figure 1 shows a typical electric field power spectral density spectrogram from the Cassini Radio and Plasma Waves Science (RPWS) instrument [*Gurnett et al.*, 2004; *Gurnett et al.*, 2005], covering nine days from March 14 to March 23, 2007. The intense broadband emission from a few tens of kHz to several hundred kHz is SKR. In the lower half of the spectrogram, narrowband emissions occur around 5 and 20 kHz periodically. An emission somewhat similar to Saturn narrowband emissions but at higher frequency occurs at Jupiter and is called Jovian narrowband kilometric emission (nKOM) [*Warwick et al.*, 1979; *Kaiser and Desch*, 1980; *Reiner et al.*, 1993; *Louarn et al.*, 2007]. Both Saturn narrowband emissions and nKOM have a relatively narrow bandwidth and are observed to recur for many consecutive planetary rotations. Another similar emission is the terrestrial continuum radiation trapped within the low density region between the plasmapause and the magnetopause [*Gurnett*, 1975]. However, unlike Saturn narrowband emission and Jovian nKOM, the terrestrial continuum radiation is not modulated at the rotational period of the Earth.

[4] *Gurnett et al.* [1981] proposed that Saturn narrowband emissions are mode converted from electrostatic waves in regions of steep plasma density gradients (i.e. on the edges of the plasma torus) via either a linear [*Jones*, 1976] or a nonlinear [*Melrose*, 1981] mechanism. *Ye et al.* [2009] modeled the source location of Saturn narrowband emissions based on the mode conversion theory, in which the narrowband emissions are mode converted from electrostatic upper hybrid waves when the matching condition $f_{UH} = (n + 1/2)f_{ce}$ is satisfied, where $f_{UH} = \sqrt{f_{pe}^2 + f_{ce}^2}$ is the local upper hybrid frequency; f_{pe} is the local plasma frequency; f_{ce} is the local electron cyclotron frequency and n is a positive integer. Evidence based on direction finding measurement and direct crossing through the source of the narrowband emissions by

[1]Department of Physics and Astronomy, University of Iowa, Iowa City, Iowa, USA.
[2]Space Research Institute, Austrian Academy of Sciences, Graz, Austria.
[3]Observatoire de Paris, Meudon, France.

0148-0227/10/2009JA015167

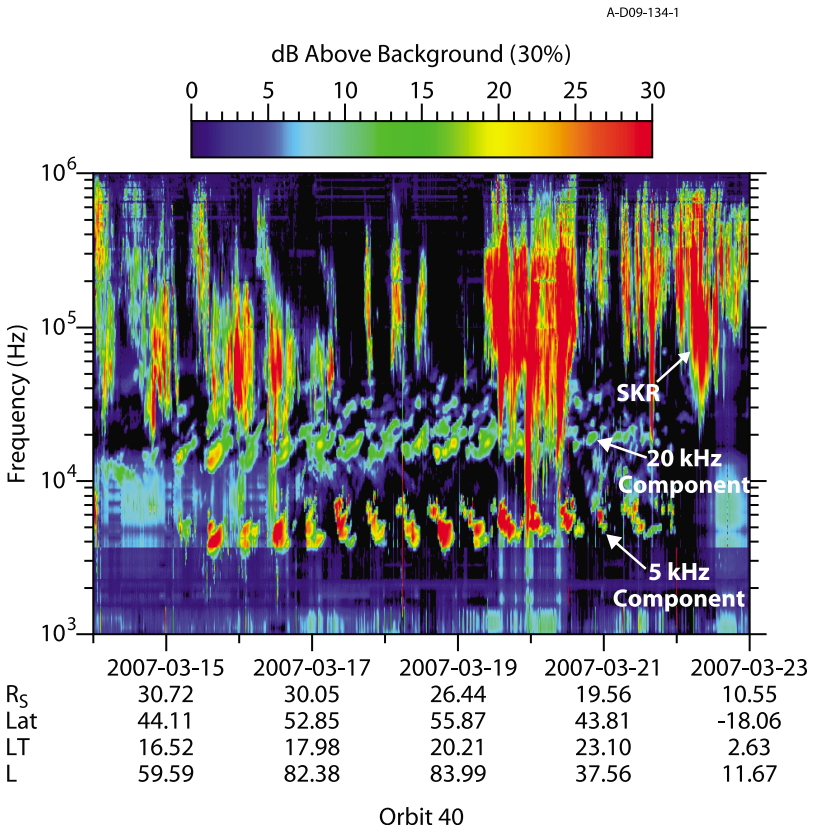

Figure 1. A typical wave electric field power spectrogram of Cassini RPWS. Narrowband radio emissions can be seen around 5 and 20 kHz as indicated by arrows.

the spacecraft shows that the generation of the 20 kHz narrowband emissions is consistent with the mode conversion theory [*Ye et al.*, 2009]. *Menietti et al.* [2009] analyzed one example of 20 kHz narrowband emission near a possible source region. Their wave growth calculation based on in-situ electron distribution measurements showed excitation of electromagnetic Z mode waves by the cyclotron maser instability, when the local upper hybrid frequency is close to nf_{ce} (n = 2, 3, …). In contrast, for the 5 kHz narrowband emissions, no source crossing has been observed in the region predicted by the *Ye et al.* [2009] model. Additionally, when Cassini is close to the planet, the measured direction of arrival for the 5 kHz narrowband emissions point to the polar region. This is not consistent with the mode conversion theory, where the narrowband emissions were postulated to originate from electrostatic upper hybrid waves within the plasma torus.

[5] In this paper, we present new evidence on the location of the source of 5 kHz Saturn narrowband emissions based on the data from Cassini RPWS instrument. In section 2, we first describe the details of the Cassini/RPWS High Frequency Receiver (HFR) which is involved in the study of narrowband emissions. In section 3, we introduce the concept of apparent polarization of radio waves measured by the RPWS/HFR. In section 4, we perform a statistical analysis of the 5 kHz narrowband emission intensities and polarizations. In section 5, we show that the direction of arrival of 5 kHz narrowband emission points to a source in the polar regions of Saturn's magnetosphere. In section 6, we report observations of 5 kHz narrowband Z mode emissions at high latitudes near perikrone. We propose that the 5 kHz narrowband radio emissions are mode converted from these Z mode emissions.

2. Cassini RPWS High Frequency Receiver

[6] Saturn narrowband emissions are mainly measured by band A (3.5–16 kHz) and B (16–71 kHz) of the RPWS/HFR [*Gurnett et al.*, 2004]. The RPWS has three 10-meter long electric antenna elements, labeled E_u, E_v and E_w. Two of the three elements (E_u and E_v) are mounted on the instrument with an angle of 120° between them, and the third element (E_w) is mounted perpendicular to the plane formed by the first two elements. The HFR can be operated in either 2-antenna (dipole-monopole) mode or 3-antenna/direction finding (DF) mode. In the 2-antenna (dipole-monopole) mode, E_u and E_v are used as a dipole E_x and two auto correlations of E_x and E_w ($\langle V_x V_x^* \rangle$ and $\langle V_w V_w^* \rangle$), and the real and imaginary parts of the cross correlation between E_x and E_w are measured ($Re\langle V_x V_w^* \rangle$ and $Im\ \langle V_x V_w^* \rangle$). In the 3-antenna/direction finding (DF) mode, E_u and E_v are used as monopoles. In this case two consecutive sets of auto and cross correlations are measured between the E_u/E_v and E_w antennas. The auto and cross correlations between the antenna voltages are measured directly in flight for each frequency channel of the HFR, with the units of the measurements in V^2/Hz.

[7] Measurements from the three electric antennas using the HFR allow us to determine the direction of arrival, the Poynting flux (S) and the polarization of a radio wave using

the analytical inversion methods provided by *Lecacheux* [2000] and *Cecconi and Zarka* [2005]. This is the so-called goniopolarimetric (from *gonia*, Greek for angle) capability [*Cecconi et al.*, 2009; *Fischer et al.*, 2009]. The polarization is usually described by the Stokes parameters Q, U, V, with Q and U denoting the linear polarization and V the circular polarization [*Kraus*, 1986]. The direction-finding inversion involves expressing the 6 wave parameters (S, Q, U, V, θ and ϕ) as functions of the antenna measurements (θ and ϕ are the colatitude and azimuth angle of the direction of arrival in the spacecraft frame) [*Cecconi and Zarka*, 2005]. In the 3-antenna (DF) mode of operation, no assumptions are necessary to perform direction finding because the number of measurements (7 independent measurements since the auto correlation of E_w is measured twice) exceeds the 6 unknown parameters. Therefore, the 3-antenna mode measurements allow us to characterize the full polarization as well as the direction of arrival of an incoming radio wave. On the other hand, in the frequently-used 2-antenna mode where we have only 4 antenna measurements but 6 parameters to solve for in the equations, assumptions have to be made for two of the six wave parameters. We must either make assumptions concerning the source direction (θ and ϕ) or the linear polarization (Q and U) of the radio waves. In the first case, also known as *polarimeter inversion*, the source is often assumed to be Saturn when the spacecraft is relatively far away from the planet. In the second case, also known as *circular goniometer inversion*, it is assumed that the radio wave has no linear polarization (i.e., $Q = 0$ and $U = 0$). This inversion will be further discussed and applied in section 5.

3. Real and Apparent Polarization Measurement

[8] The real polarization of a radio wave is given by the Stokes parameters which are defined via the wave electric field components in the wave plane, which is the plane perpendicular to the wave vector. However, the wave vector information is not always available, for example in the 2-antenna mode that is often used during the Cassini mission, where assumptions have to be made on the linear polarization of radio waves in order to retrieve the propagation direction. Due to this, we introduce the concept of apparent polarization, which is given by the apparent Stokes parameters S_{app}, q_{app}, u_{app} and v_{app} defined by the wave electric field components measured by the two orthogonal antennas in the antenna plane.

$$S_{app} = \frac{1}{Z}\left(\frac{\left\langle V_x V_x^* \right\rangle}{h_x^2} + \frac{\left\langle V_w V_w^* \right\rangle}{h_w^2}\right) \tag{1}$$

$$q_{app} = \frac{1}{ZS_{app}}\left(\frac{\left\langle V_x V_x^* \right\rangle}{h_x^2} - \frac{\left\langle V_w V_w^* \right\rangle}{h_w^2}\right) \tag{2}$$

$$u_{app} = \frac{1}{ZS_{app}}\frac{2Re\left\langle V_x V_w^* \right\rangle}{h_x h_w} \tag{3}$$

$$v_{app} = \frac{1}{ZS_{app}}\frac{2Im\left\langle V_x V_w^* \right\rangle}{h_x h_w} \tag{4}$$

where V_x and V_w are the voltages induced by an electromagnetic wave on the E_x and E_w antennas, and h_x and h_w are the effective lengths of the two antennas. Z is the intrinsic impedance of the medium [*Kraus*, 1953], which is $120\pi\ \Omega$ for vacuum. The asterisk * denotes the complex conjugate, and the brackets $\langle \ldots \rangle$ represent the averaging operation over the integration time. The formulas for calculating the apparent Stokes parameters are derived in Appendix A of *Fischer et al.* [2009]. It should be noted that q_{app}, u_{app} and v_{app} are normalized apparent Stokes parameters, which are divided by the apparent Poynting flux S_{app}, and therefore are scalars ranging from −1 to +1 with no physical units. The apparent circular polarization degree is defined as $d_{c,app} = v_{app}$, with $v_{app} = +1$ indicating a left hand circularly polarized wave and $v_{app} = -1$ indicating a right hand circularly polarized wave. The apparent linear polarization degree is defined as $d_{l,app} = \sqrt{q_{app}^2 + u_{app}^2}$, with $d_{l,app} = 1$ indicating a linearly polarized wave. The apparent total polarization degree is defined as $d_{app} = \sqrt{q_{app}^2 + u_{app}^2 + v_{app}^2}$, with $d_{app} = 0$, 0.5 and 1 indicating an unpolarized, partially polarized, and completely polarized wave, respectively. The real polarization should be calculated from the apparent Stokes parameters by a linear transformation [*Hamaker et al.*, 1996; *Galopeau et al.*, 2007] where the incoming wave direction is assumed to be known.

[9] *Fischer et al.* [2009] showed that the relation between the signs of the real and apparent circular polarization degree is dependent on the wave incident angle β with respect to the antenna plane. For $\beta > 0$, we have $sign(v) = sign(v_{app})$, whereas for $\beta < 0$, $sign(v) = -sign(v_{app})$. In the frequently used 2-antenna mode, $\beta > 0$ corresponds to the hemisphere on the magnetometer boom side of the $E_x - E_w$ antenna plane, whereas $\beta < 0$ corresponds to the hemisphere on the ISS (Imaging Science Subsystem) side of the $E_x - E_w$ antenna plane. In case the radio source crosses the antenna plane due to a spacecraft rotation, there will be a sign flip in the apparent circular polarization. When Cassini is not rotating, ISS is pointed toward Saturn most of the time, so we have $\beta \cong -60$ deg, assuming the radio emissions are coming from the direction of Saturn. This means that a circularly polarized wave will appear to have a polarization sense opposite to that of the real one. As discussed by *Ye et al.* [2009] the real polarization of a wave is determined by both its magnetoionic mode and beaming angle, i.e. the angle between $\mathbf{k}$ and $\mathbf{B}$. The magnetoionic mode determines the polarization sense of a wave with respect to the local magnetic field at the source. In the absence of plasma effects, the circular polarization sense of a radio emission with respect to the wave vector $\mathbf{k}$ (real) will remain the same after it leaves the source region[*Gurnett et al.*, 1988]. So if $\mathbf{k} \cdot \mathbf{B} > 0$, the real polarization (defined with respect to $\mathbf{k}$) sense will be the same as the polarization sense of the magnetoionic mode at the source (with respect to $\mathbf{B}$); whereas if $\mathbf{k} \cdot \mathbf{B} < 0$, the real polarization sense will be opposite to that of the magnetoionic mode at the source. For example, the real circular polarization sense of the right-hand extraordinary (R-X) mode SKR is right hand in the Northern Hemisphere ($\mathbf{k} \cdot \mathbf{B} > 0$) and left hand in the Southern Hemisphere ($\mathbf{k} \cdot \mathbf{B} < 0$) [*Lamy et al.*, 2008]. If ISS is pointing to Saturn, the R-X mode emission would appear, to the antenna plane, to be left-hand polarized in

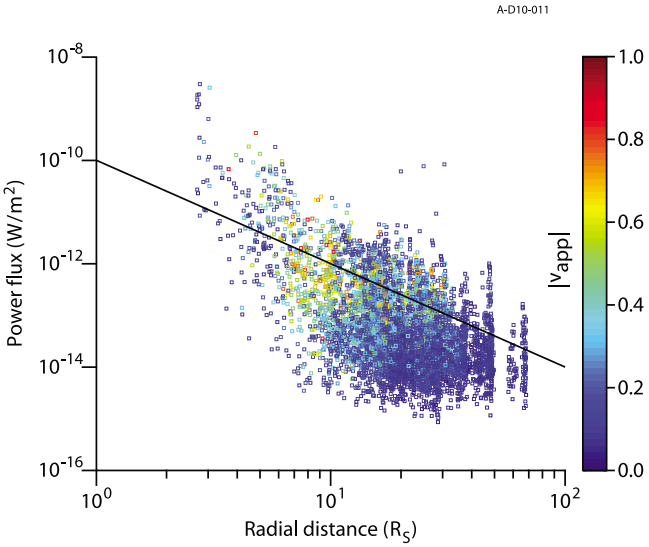

Figure 2. The power flux of 5 kHz narrowband emissions (S_{app} integrated from 3 to 7 kHz and then averaged over 1-hour period) versus the radial distance of Cassini. The color of the dots indicate the averaged absolute value of the apparent circular polarization degree (v_{app}, defined in section 3). The straight line represents a $1/R^2$ dependence of the wave power.

the Northern Hemisphere and right-hand polarized in the Southern Hemisphere.

4. Source Location Indicated by Region of Occurrence

[10] Since Cassini's arrival at Saturn in 2004, narrowband emissions have been frequently detected by the RPWS instrument. *Farrell et al.* [2005] showed 3–70 kHz Z mode narrowband emissions detected during Saturn orbit insertion (SOI) at a radial distance less than 2.5 R_S (Saturn Radius = 60,268 km). Their reason for identifying the waves with the Z mode was that the narrowband emission propagates through local f_{pe} and its low frequency cutoff is at the L = 0 cutoff, $f_{L=0} = -\frac{f_{ce}}{2} + \sqrt{\frac{f_{ce}^2}{4} + f_{pe}^2}$ [*Gurnett and Bhattacharjee*, 2005]. *Louarn et al.* [2007] compared the 5 kHz narrowband emissions (n-SMR or narrowband Saturn myriametric radiation in their terminology) with the Jovian nKOM (narrowband kilometric radiation) and proposed that the source of these emissions is located at either the inner ($L \sim 2$) or the outer ($L \sim 10$ to 12) boundary of the plasma disk near the equatorial plane. More recently, *Wang et al.* [2010] associated the occurrence of the 5 kHz Saturn narrowband emissions with energetic plasma injections, which are indicated by ENA (energetic neutral atoms) brightening events detected by MIMI/INCA (Magnetospheric Imaging Instrument/Ion and Neutral Camera) [*Krimigis et al.*, 2004]. They further estimated, based on the mode conversion theory, that the source locations for 5 kHz narrowband emissions are on the northern and southern boundaries of the plasma torus at L-shells of 7 to 8.

[11] To resolve the uncertainty in the location of Saturn narrowband radio emissions, we follow the method *Gallagher and Gurnett* [1979] used to determine the time-averaged source location for auroral kilometric radiation (AKR) at Earth. In Figure 2, the averaged power flux of 5 kHz narrowband emissions detected by RPWS/HFR from day of year (DOY) 134, 2005 to DOY 298, 2009 is plotted versus the radial distance of Cassini. The power flux of the 5 kHz narrowband emissions, calculated by integrating the apparent Poynting flux S_{app} over the frequency range 3–7 kHz, is averaged over one-hour periods. The color of the dots shows the averaged absolute value of the apparent circular polarization degree $|v_{app}|$ of the emissions. Note we only show the magnitude of the apparent circular polarization here, so the rotation sense is ignored.

[12] As the radial distance R of Cassini increases, the power of the 5 kHz narrowband falls roughly as $1/R^2$ (i.e. the power falls by 4 orders of magnitude as the distance increases by 2 orders of magnitude). The straight line in Figure 2 represents a $1/R^2$ dependence of the wave power. The most intense emissions at 5 kHz are observed around 3 R_S. However, the absolute values of the apparent circular polarization degree of these emissions are mostly low, which normally means that these emissions are either linearly polarized (a necessary but not sufficient condition for electrostatic waves) or unpolarized (likely due to a superposition of electromagnetic waves from numerous random sources). We found no linear polarization component for the narrowband emissions. So for narrowband emissions with low $|v_{app}|$, the total polarization degree is low (close to unpolarized). Highly polarized narrowband emissions begin at around 6 R_S, indicating a possible mode transition to radio waves. So we propose that the 5 kHz narrowband emissions are generated within 6 R_S. It should be noted that at high latitudes, the local electron cyclotron frequency f_{ce} at 6 R_S is about 5 kHz, which means that most of the 5 kHz narrowband emissions are excited below the local f_{ce}.

[13] Figure 3 shows color-coded trajectories of Cassini in the meridian plane for the five years from DOY 134, 2005 to DOY 298, 2009. In the top plot, the color of the trajectories represents the dB level of the power flux of the 5 kHz narrowband emissions. Each value of the power flux, an integration of apparent Poynting flux S_{app} over the frequency range 3–7 kHz, is averaged over one hour intervals. In the bottom plot, the color represents the absolute value of the apparent circular polarization degree $|v_{app}|$ averaged over the same time and frequency interval. The plots show that the most intense 5 kHz narrowband emissions are observed interior to the plasma torus, and the emissions with high absolute values of circular polarization degree are observed only in the high latitude regions.

5. Direction Finding Results

[14] As discussed in section 2, in the circular goniometer inversion, we assume no linear polarization (i.e., $Q = 0$ and $U = 0$), and we can retrieve the direction of arrival (θ and ϕ), Poynting flux S and the circular polarization V of the radio waves. This inversion has been used in the statistical study of SKR properties [*Lamy et al.*, 2008] and the case study of SKR source locations [*Cecconi et al.*, 2009]. The narrowband emissions have been found to be purely circularly polarized at high latitudes but partially polarized or unpolarized at low latitudes with no linear component [*Ye et al.*, 2009], which justifies the use of the 2-antenna direction inversion at least

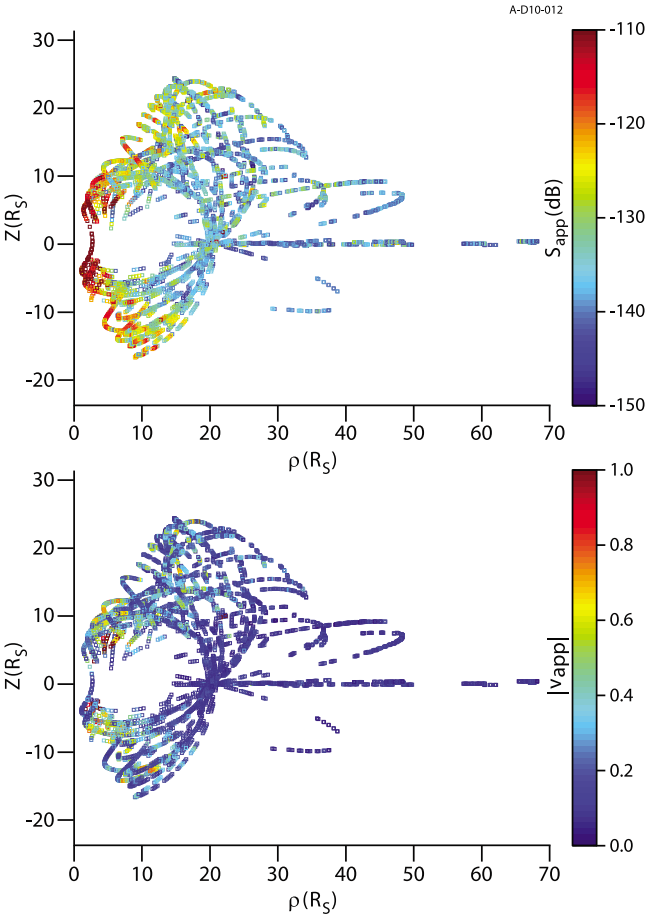

Figure 3. Color coded trajectories of Cassini when 5 kHz narrowband emissions are observed (in a meridian view). (top) The color of each dot indicates the dB level of averaged apparent Poynting flux of 5 kHz narrowband emissions. (bottom) The color of each dot indicates the averaged absolute value of apparent circular polarization degree (v_{app}, defined in section 3) of 5 kHz narrowband emissions.

at high latitudes. The 2-antenna mode can give the direction of arrival to the source, provided the polarization assumption is valid. It has also been shown by *Ye et al.* [2009] that the results of the 3-antenna and the 2-antenna direction inversion methods are consistent with each other.

[15] Figure 4 (top) shows an electric field power spectrogram of Cassini RPWS data on DOY 343–344, 2008. The spacecraft was at relatively high latitude (>70°) when the narrowband emissions were observed. The spacecraft radial distance changed from 12 R_S to 9 R_S over the time range of the spectrogram. We determine the source location of the 5 kHz narrowband emissions (from 2300 to 2400 SCET, DOY 343, 2008) using the 2-antenna direction finding results. A 3D perspective of the source location of the 5 kHz narrowband emissions is shown in Figure 4 (bottom). In Figure 4 (bottom), the locations of the spacecraft are represented by black diamonds. The red rings are the modeled source locations of the 5 kHz narrowband emissions based on the assumption that the narrowband emissions are mode converted from electrostatic upper hybrid waves on the outer boundary of the plasma torus [*Ye et al.*, 2009]. The locations of these rings are determined by the matching condition $f_{UH} = (n + 1/2)f_{ce}$, with $n = 1$. The multiple rings are due to the finite bandwidth (4–6 kHz) of 5 kHz narrowband emissions. There are multiple frequency channels of the HFR within this frequency range. Each ring corresponds to a modeled source location for a particular frequency channel. The purple dots are the interception points of the direction of arrival and the planes that contain the modeled source rings. The green dots are the interception points of the direction of arrival and the f_{ce} = 5 kHz surface. From the perspective of the spacecraft, the 5 kHz narrowband emissions appear to have a source in the auroral zone of Saturn rather than near the outer boundary of the plasma torus as first suggested by *Ye et al.* [2009] and *Wang et al.* [2010].

6. Z Mode Narrowband Emissions Observed at High Latitude Perikrone

[16] In 2008, Cassini shifted to very high latitude orbits up to 75°. When the spacecraft was within a radial distance of 6 R_S, where $f_{ce} \geq 5$ kHz, intense narrowband emissions were observed below f_{ce} (white curves in Figures 5–7). In this underdense region, where f_{pe} is much lower than f_{ce}, f_{ce} is very close to f_{UH}.

[17] Figure 5 shows the wave electric field power and apparent polarization spectrograms of Cassini RPWS on DOY 168, 2008. During the day, Cassini moved from high northern latitude to high southern latitude. As described in section 3, the apparent sense of circular polarization, which is given by the sign of v_{app}, can be linked to the real sense of circular polarization v of the received wave. On one side of the antenna plane the apparent sense equals the real sense, whereas on the other side the apparent sense is opposite to the real sense. This is why the apparent sense of polarization switches its sign when the source crosses the antenna plane as can be seen in Figure 5 by the sudden switches in apparent circular polarization v_{app} of SKR from about 02:00 to 09:00 SCET on DOY 168, 2008. When the L-O mode narrowband emission is observed somewhat later around 15:00 UT, we know from Cassini attitude data that Saturn and hence the sources of SKR and narrowband emissions are located on the side of the antenna plane where the apparent sense is opposite to the real sense of polarization. It is shown by *Lamy et al.* [2008] that SKR propagates mainly in the R-X mode. The R-X mode SKR observed from the Southern Hemisphere is in fact left-hand polarized ($v > 0$) since at the source the magnetic field and the direction of wave propagation are opposite to each other. Hence, the apparent polarization of SKR is right-handed ($v_{app} < 0$) due to the position of Saturn with respect to the antenna plane. This is just the opposite for the narrowband emission above local f_{ce} because it is L-O mode. The same is true for Figures 6 and 7 for the times when Cassini is cruising in the Southern Hemisphere. In almost all cases the narrowband emissions above local f_{ce} are observed to be oppositely polarized to SKR, which in fact means that those two types of freely propagating electromagnetic emission must be attributed to different modes. (The exceptional case of L-O mode SKR can be seen in Figure 6 around 12:00 UT and 100 kHz.)

[18] In Figure 5, between 13:00 and 14:00 SCET (marked by the closed dashed line), the 5 kHz narrowband emission crossed the local f_{ce}. The intensity of the 5 kHz narrowband

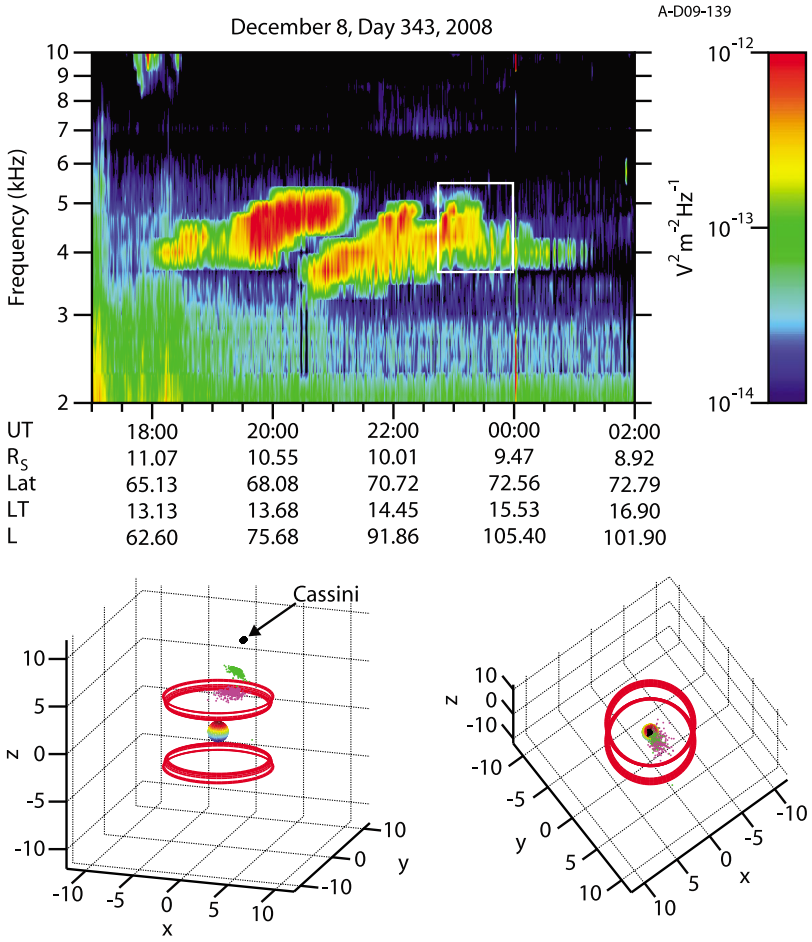

Figure 4. (top) Cassini RPWS electric field power spectrogram on DOY 343–344, 2008, and (bottom) RPWS 2-antenna direction finding results of the 5 kHz narrowband emissions observed between 2300 and 2400 SCET on DOY 343, 2008. The black diamond dot is the location of the spacecraft. The rings (corresponding to different frequency channels within the bandwidth 4–6 kHz) are the modeled source locations for 5 kHz narrowband emissions based on *Ye et al.* [2009]. The purple dots are the interception points of the directions of arrival and the planes that contain the modeled source rings. The green dots are the interception points of the direction of arrival and the f_{ce} = 5 kHz surface. The results are shown from both side and spacecraft perspectives.

emissions dropped by about 20 dB from below f_{ce} to above f_{ce} (Figure 5 (top)). The apparent circular polarization of the 5 kHz narrowband emissions also switched from right hand (similar to SKR) below local f_{ce} to left hand (opposite to SKR) above local f_{ce} (Figure 5 (middle)). During the crossing of the 5 kHz iso-f_{ce} surface, the spacecraft was not rotating, so the apparent polarization reversal was not due to the radio source crossing the antenna plane. Rather, the change in polarization sense at local f_{ce} suggest a mode change from a right-hand polarized mode to the L-O mode. Note also that the apparent total polarization degree of the 5 kHz narrowband emissions is <1 below local f_{ce} and ~1 above local f_{ce} (Figure 5 (bottom)).

[19] Figure 6 shows the Cassini RPWS data on DOY 121, 2008 in the same format as that of Figure 5. Note the intensity drop and apparent circular polarization reversal of the 5 kHz narrowband emission at local f_{ce} between 20:00 and 22:00 SCET (marked by the closed dashed line in Figures 6 (top) and 6 (middle)). In the bottom panel, the apparent total polarization degree of the 5 kHz narrowband emission is ~1 both above and below the local f_{ce}. It is interesting that the 5 kHz narrowband emission has a gap along the local f_{ce}, where the total polarization degree is ~0. This gap will be discussed later.

[20] We identify the right hand polarized 5 kHz narrowband emission observed below local f_{ce} with Z mode waves. These Z mode narrowband emissions can mode convert and escape as L-O mode narrowband emissions as normally observed above local f_{ce}. The dispersion relation diagrams from *Sonwalkar et al.* [2004, Figure 1] show the wave frequency as a function of the wave vector **k** as well as the polarization for different wave modes. In the underdense case ($f_{pe} < f_{ce}$), Z mode is in the R-X mode. Between f_{pe} and f_{UH}, which is close to f_{ce}, both Z mode and L-O mode narrowband emissions can exist. If the L-O mode narrowband emissions are mode converted from Z mode waves, the intensity of the L-O mode would be much less than the Z mode. Therefore, the polarization as measured by Cassini should

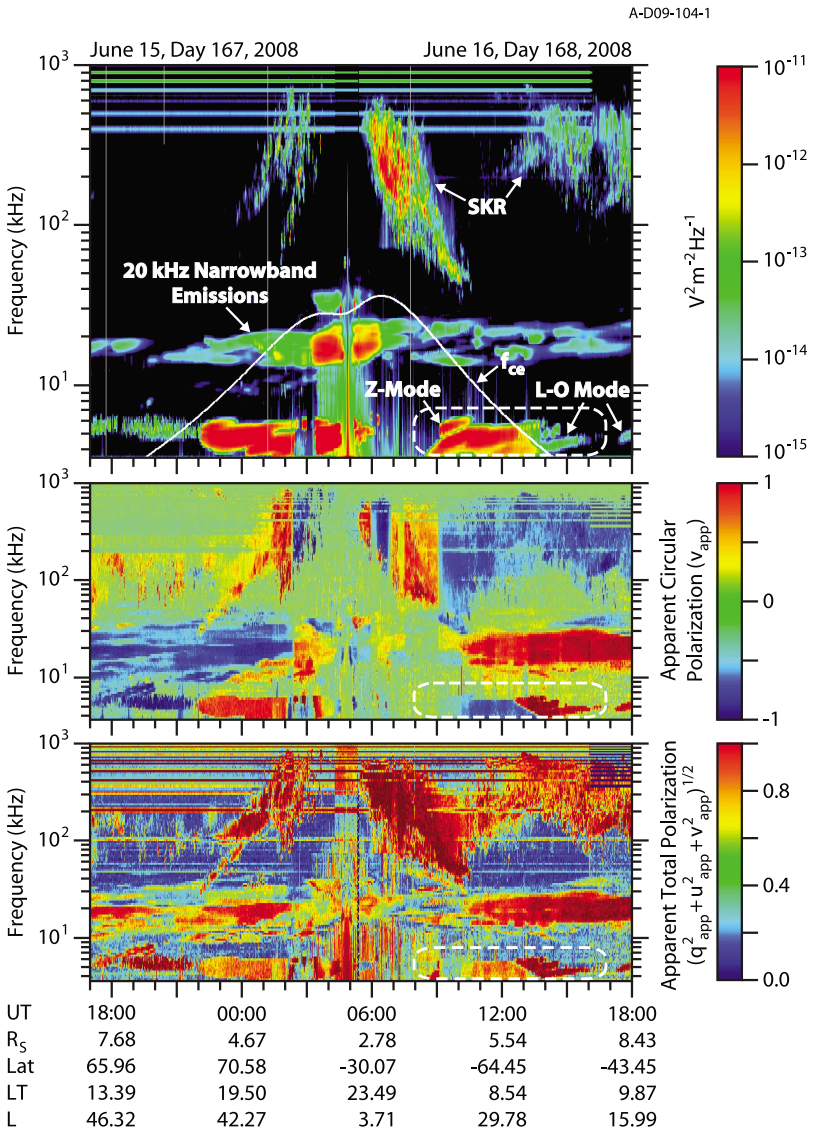

Figure 5. Wave electric field power and polarization spectrograms of Cassini RPWS on DOY 168, 2008. (top) The intensity, (middle) the apparent circular polarization, and (bottom) displays the apparent total polarization.

be dominated by the Z mode. The Z mode wave terminates at f_{UH} while the L-O mode can propagate above f_{UH}. So above $f_{UH} \sim f_{ce}$, only the L-O mode narrowband emissions can propagate. Below f_{ce}, the polarization of narrowband emissions is consistent with the Z mode with total polarization degrees somewhat lower than 1. The low total polarization degree could result from multiple reflections of the waves due to trapping of Z mode waves between the boundaries set by f_{UH} and $f_{L=0}$ surfaces (as shown later in Figure 9). A mixture of electromagnetic waves propagating in different directions would appear partially polarized. Note in the lower panel of Figure 6 (also seen in Figure 5) that we have a tiny gap between left-hand and right-hand polarized narrowband emissions, where the total polarization degree is close to zero. This gap might correspond to the frequency gap between f_{ce} and f_{UH}, where Z mode waves propagate on the resonance cone and become quasi-electrostatic [*Gurnett et al.*, 1983], leading to the low total polarization degree.

[21] Figure 7 shows the wave electric field power and apparent polarization spectrograms on DOY 291, 2008. The mode conversion of the 5 kHz narrowband emissions from Z mode to L-O mode is observed around −74° latitude. Notice the source crossing of the SKR around 0900 SCET, which is identified by the frequencies of SKR being extended to slightly below the local f_{ce}. The fact that Z mode narrowband emissions are preferably observed in the high latitude region (see Figure 9 and Table 1) and sometimes near the source of SKR seems to suggest a possible auroral source for 5 kHz narrowband emissions. An auroral source of narrowband emissions is also consistent with the direction finding result shown in section 5, where the direction of arrival points to the polar region. Figure 8 shows the only RPWS wide-band data for the 3-hour long interval when the 5 kHz narrowband emissions changed circular polarization sense

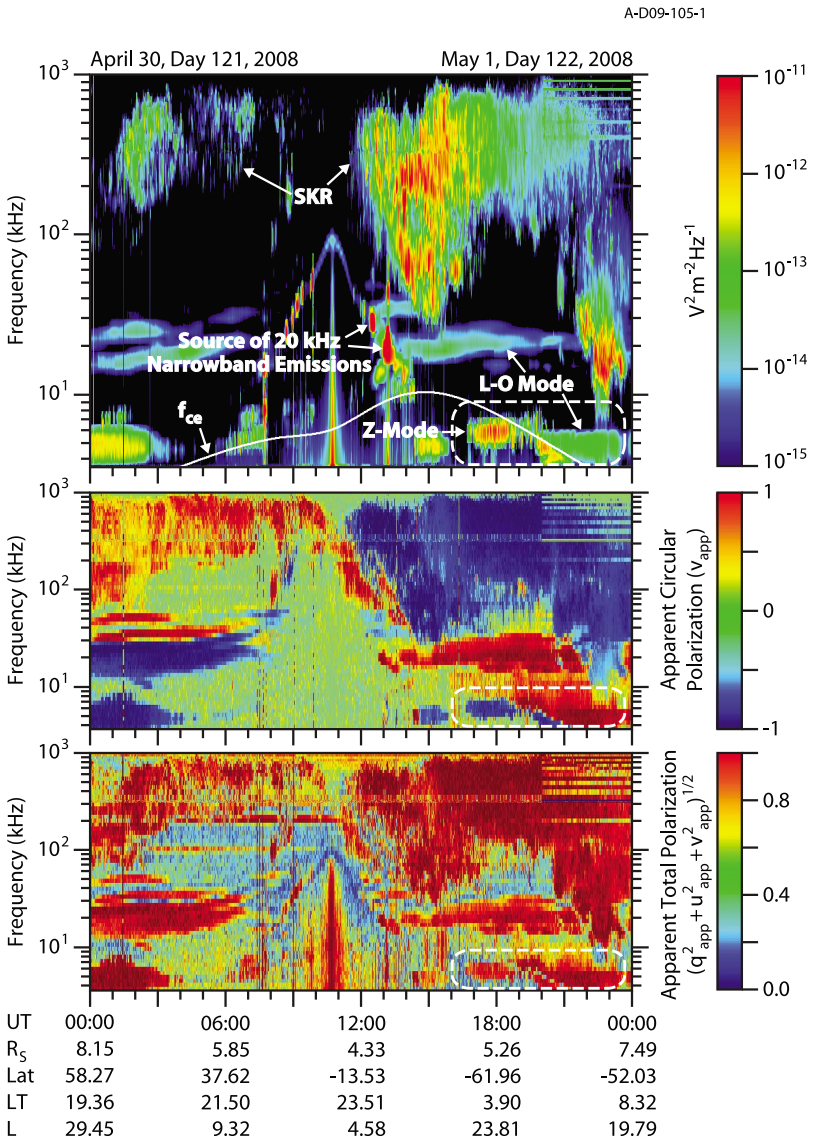

Figure 6. Wave electric field power and polarization spectrograms of Cassini RPWS on DOY 121, 2008, in the same format as Figure 5.

at local f_{ce} (as shown in Figure 7 (middle)). The wide-band receiver data shown in Figure 8 reveals an interesting fine frequency-time structure (vertical stripes) shared by the Z mode below local f_{ce} and the L-O mode above f_{ce}. It is also shown that as the 5 kHz narrowband emission goes from below to above the local f_{ce}, the fine structure of the Z mode persists in the L-O mode emission whereas the intensity drops by about 20 dB just before the crossing of the local f_{ce}. This indicates a common source for the Z mode and L-O mode waves. The weaker L-O mode emission, which has only ~1% of the wave energy of the Z mode waves, might be the result of a mode conversion from the much more intense Z mode waves.

[22] In Table 1, we list the time and location of events in which apparent circular polarization reversals of 5 kHz narrowband emissions are observed at the local f_{ce}. Notice that most of these polarization reversals are observed at relatively high latitudes. We will show later that the positions of Cassini at the time of the polarization reversals are located practically at the f_{ce} = 5 kHz contour. The observation of polarization reversal at the local f_{ce} favors the dawn and dusk sectors as indicated by the local time distribution of the events. The implication of this local time preference is still unclear. We also investigated the polarization characteristics of all those reversals and found the narrowband emission to be polarized like SKR below the local f_{ce} and polarized in the opposite sense to SKR above the local f_{ce}.

7. Discussion

[23] Narrowband events like those shown in Figures 5, 6 and 7 have been observed at other planets. Using the wave instrument onboard DE-1 in orbit around Earth, *Hashimoto and Calvert* [1990] detected L-O mode/Z mode waves immediately above/below the local f_{ce} at 60–70° magnetic latitude. Similarly, Ulysses/URAP observed polarization

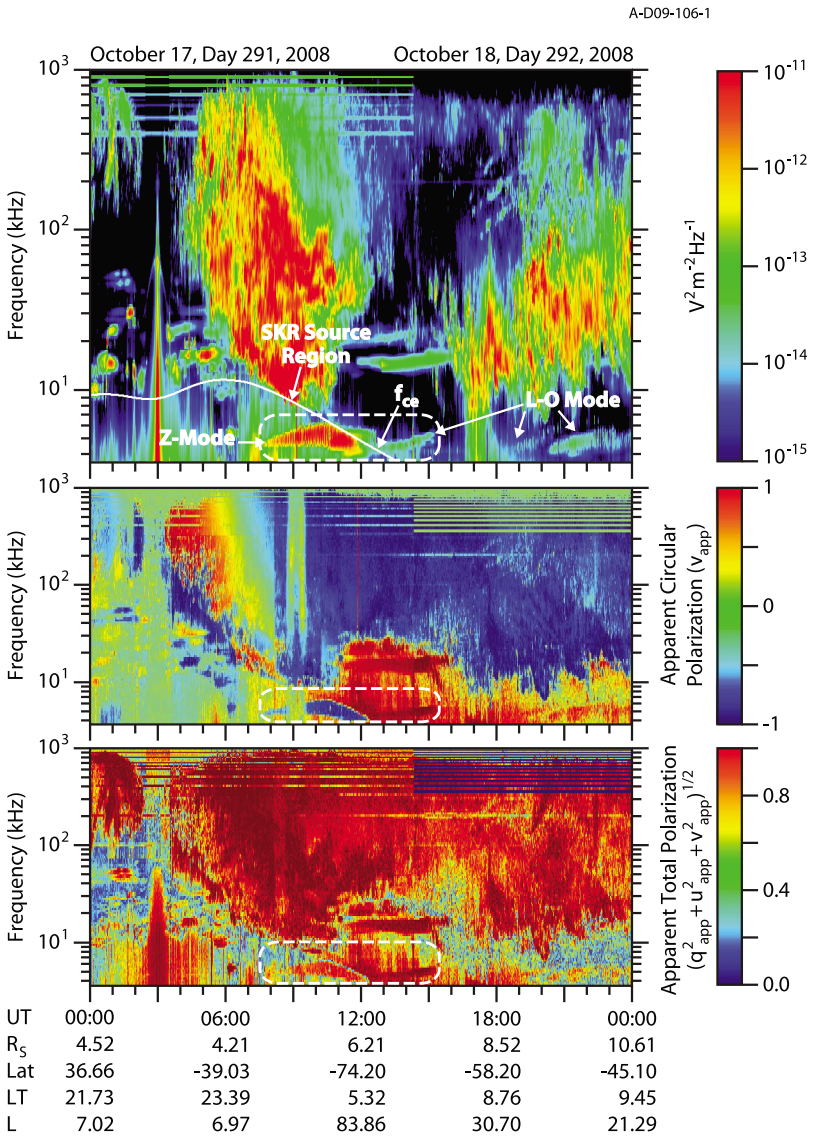

Figure 7. Wave electric field power and polarization spectrograms of Cassini RPWS on DOY 291, 2008. A transition of 5 kHz narrowband emissions from Z mode to L-O mode can be seen around 1100 SCET.

reversal of radio emissions in the polar region of Jupiter [*Kaiser et al.*, 1993]. Galileo/PWI also observed a mode change from Z mode to L-O mode across the local f_{ce} at low latitudes interior to the Io plasma torus [*Menietti et al.*, 2005]. All these observations indicate that the polarization reversal of radio emissions due to the mode conversion from Z mode to L-O mode around the local f_{ce} is a common phenomenon at all planets with magnetospheric radio emissions.

[24] The Z mode narrowband emissions can be generated in three different ways: 1. mode conversion from electrostatic upper hybrid waves [*Oya and Morioka*, 1983; *Perraut et al.*, 1998]; 2. mode conversion from Langmuir waves [*Farrell et al.*, 2005]; and 3. direct generation by the cyclotron maser instability [*Yoon et al.*, 1998; *Menietti et al.*, 2009]. *Oya and Morioka* [1983] proposed a mode conversion theory for the generation of L-O mode AKR. In this theory, electrostatic upper hybrid waves in the source region are converted into Z mode waves that propagate toward dense plasma regions where the wave frequency is equal to the local plasma frequency, where part of the wave energy is transferred to the L-O mode. These free space propagating L-O mode waves are then observable by the spacecraft far away from the source. *Perraut et al.* [1998] attempted to identify the source of the L-O mode emissions detected outside the Jovian plasma sheet. They proposed that the quasi-electrostatic waves observed below the upper hybrid frequency are successively mode converted into Z and later L-O mode. This is similar to the linear conversion theory invoked by *Jones* [1976, 1980] to explain the terrestrial myriametric and Jovian narrowband kilometric radiations. *Farrell et al.* [2005] proposed that the narrowband Z mode emissions observed at Saturn during SOI are generated by mode conversion from intense Langmuir waves at a density gradient parallel to the local magnetic field. *Yoon et al.* [1998] and *Menietti et al.*

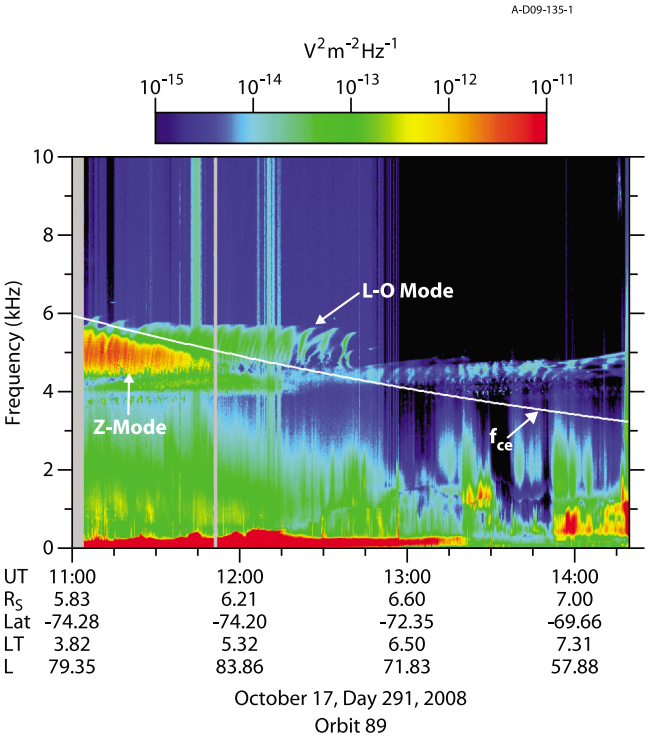

Figure 8. Wide-band receiver data of Cassini RPWS from 1100 to 1420 SCET on DOY 291, 2008. A sharp drop in power of the 5 kHz narrowband emissions can be seen at local f_{ce} between 1100 and 1200 SCET.

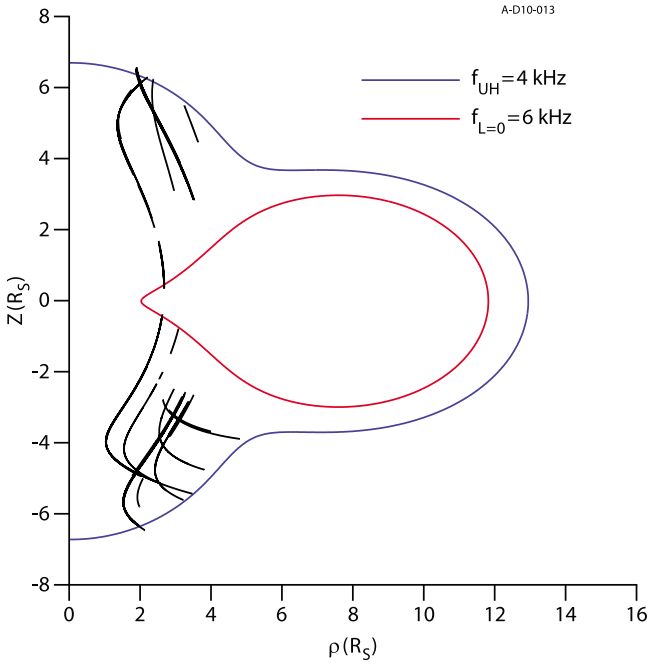

Figure 9. Possible source location of 5 kHz Z mode narrowband emissions based on an electron density model of the plasma torus in the meridian plane. The red and blue contour lines represent $f_{L=0}$ = 6 kHz and f_{UH} = 4 kHz respectively. The black lines show the Cassini positions when the 5 kHz Z mode narrowband emissions are observed.

[2009] showed that the Z mode emissions can also be directly generated by the cyclotron maser instability, when the local upper hybrid frequency is close to multiples of the local electron cyclotron frequency ($f_{UH} \cong nf_{ce}$).

[25] Although there is still uncertainty about the source location of the 5 kHz Z mode narrowband emissions, we know that the Z mode waves are trapped between f_{UH} and the L = 0 cutoff and cannot escape from Saturn [*Gurnett et al.*, 1983]. Figure 9 shows a model of the possible region where the 5 kHz Z mode narrowband emissions can propagate in the meridian plane. The blue contour line shows the boundary where f_{UH} = 4 kHz, the lower frequency limit of the 5 kHz narrowband emissions. The red contour line shows the boundary where $f_{L=0}$ = 6 kHz, the upper frequency limit of the 5 kHz narrowband emissions. The propagation of the 5 kHz Z mode narrowband emissions should be restricted between the blue and red contours. The magnetic field used in this model is the zonal harmonic (Z3) model of *Connerney et al.* [1982] and the electron density profile of the plasma torus is based on the results of *Persoon et al.* [2006]. The model suggests that the Z mode waves can propagate on the boundary of the plasma torus and the region interior to the plasma torus with the radial distance $<6R_S$. Cassini trajectories (black) where 5 kHz Z mode narrowband emissions were observed in 2008 are plotted in the same meridian plane. The locations where the 5 kHz Z mode narrowband emissions are observed, mainly in the high latitude low density region, is generally consistent with the model results. Only a small portion of the trajectories extend beyond the f_{UH} = 4 kHz line, when the frequency of narrowband emissions sometimes extends to as low as 3 kHz.

[26] *Kennel et al.* [1987] and *Barbosa et al.* [1990] analyzed the narrowband Z mode emissions detected in Jupiter's magnetosphere. These emissions are separated from the broad band continuum radiation at higher frequency by a deep emission gap. *Barbosa et al.* [1990] associated the Z mode

Table 1. Narrowband Emissions Polarization Reversal at Local f_{ce}

Year-DOY	Time (SCET)	Latitude (deg)	Radial Distance (R_S)	LT
2008-322	0600	−70	6	5
2008-291	1100	−75	6	5
2008-290	1700	70	7	18
2008-269	1100	−75	6	6
2008-247	0800	−75	6	5
2008-231	2200	70	6	20
2008-217	0300	70	7	19
2008-210	0400	70	6	15
2008-203	0300	70	6	15
2008-196	0200	70	6	14
2008-189	0200	70	6	15
2008-182	0000	70	6	15
2008-175	1500	−65	6	9
2008-168	1300	−55	6	9
2008-167	2200	75	6	16
2008-146	1500	65	6	19
2008-138	1500	65	6	19
2008-121	2000	−60	6	7
2008-062	1200	−50	6	7
2008-052	0200	−40	5	8
2008-028	0030	−40	5	7

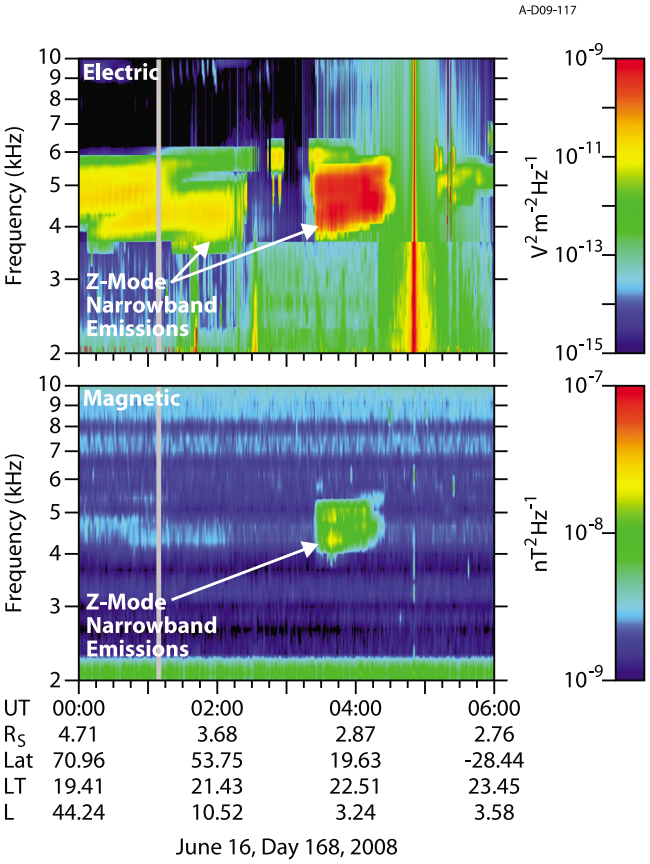

Figure 10. (top) The electric field power spectrogram of the Z mode narrowband emission observed from 0000 to 0600 SCET of DOY 168, 2008, and (bottom) the magnetic field component of this emission detected by the tri-axial search coil magnetometer of RPWS.

peak frequencies with the left hand cut-off frequencies, suggesting that the intense Z mode emission is a result of the wave reflection at the cut-off layer. These observations of Z mode waves are consistent with the scenario that upper hybrid waves on the boundary of the magnetodisc of Jupiter are the source of the continuum radiation.

[27] Simultaneous measurements using the electric and magnetic field antennas would allow us to compute the refractive index cB/E of the Z mode narrowband emissions, which can be compared to the theoretical values. Normally, narrowband emissions cannot be detected by the tri-axial search coil magnetometer, probably due to the low sensitivity of the magnetic antenna. Note the inflight noise level of the magnetic search coil at 5 kHz is around 10^{-9} nT^2/Hz [*Gurnett et al.*, 2004]). Assuming $cB/E = 1$, the narrowband emissions would have to be stronger than $10^{-10} V^2/m^2$ Hz for the magnetic component to be detected. Most of the narrowband emissions are less intense than this threshold. As a result, only a couple of events with a magnetic field component have been detected so far, probably when the spacecraft (radial distance ~2.8–2.9R_S) was very close to the source of 5 kHz narrowband emissions. Figure 10 shows an intense 5 kHz Z mode narrowband emission observed by Cassini RPWS around 0400 SCET of DOY 168, 2008. This is the first time that the magnetic field component of narrowband emissions has been reported. The electric field power spectral density of the Z mode emission was around $10^{-9} V^2/m^2$ Hz and the magnetic field power spectral density was around 10^{-8} nT^2/Hz. The resulting cB/E ratio is close to 1, indicating that the Z mode waves are propagating near the speed of light. Theoretical calculation based on the plasma frequency (f_{pe} = 6 kHz (J.-E. Wahlund and M. Morooka, personal communications, 2009)) measured by the RPWS Langmuir probe [*Gurnett et al.*, 2004] and the local electron cyclotron frequency (f_{ce} = 28 kHz) measured by the Cassini magnetometer[*Dougherty et al.*, 2004] shows that the Z mode refractive index is $n = 0.99$ for a wave frequency of 5 kHz and a wave normal angle of 89°. *Gurnett and Bhattacharjee* [2005, Figures 4.37 and 4.38] also showed that the refractive index of Z mode waves is close to 1 in all wave normal directions for wave frequencies lower than the local plasma frequency. Therefore, the theoretical value of the Z mode refractive index is consistent with the value of cB/E calculated from the electric and magnetic field measurements. This consistency further confirms the identification of the 5 kHz narrowband emission observed below f_{ce} with the Z mode.

[28] Z mode narrowband emissions detected by the Cassini RPWS during the Saturn Orbit Insertion, which *Farrell et al.* [2005] identified to be from the interior boundary of Saturn's plasma torus, are unlikely the source of L-O mode narrowband emissions. This is because their intensities ($<10^{-14}$ V^2/m^2 Hz) are less than or only comparable to the typical intensities ($10^{-14} \sim 10^{-12}$ V^2/m^2 Hz) of the L-O mode narrowband emissions observed farther from the planet.

8. Conclusions

[29] Although *Ye et al.* [2009] associated the intense electrostatic upper hybrid waves in the plasma torus of Saturn with the 20 kHz narrowband emissions, the source of the 5 kHz narrowband emissions was still unclear. However, this paper presents strong evidences that the 5 kHz L-O mode narrowband emissions originate from the narrowband Z mode emissions detected near the auroral zones in the polar region of Saturn. Statistical analysis of the five years (2005–2009) of Cassini/RPWS observation shows that the sources of 5 kHz narrowband emissions are close to the planet, with the most intense Z mode narrowband emissions observed around 3 R_S from Saturn's center. It is also found that the highly circularly polarized 5 kHz narrowband emissions are observed only in the high latitude regions, whereas the 5 kHz narrowband emissions observed near the equator are mostly unpolarized (both the circular polarization degree and the linear polarization degree are zero). The RPWS 2-antenna direction finding results for the 5 kHz narrowband emissions point to a source in the polar region. In 2008, 21 events were observed where the circular polarization of the 5 kHz narrowband emissions switches sense and the intensity drops by about 20 dB as the spacecraft crosses the f_{ce} = 5 kHz surface. The 5 kHz narrowband emissions observed below local f_{ce} are polarized similarly to SKR, and those above local f_{ce} are polarized oppositely to SKR. The observed circular polarization sense is consistent with the Z mode polarization. We propose that the escaping 5 kHz L-O mode narrowband

emissions are mode converted from Z mode narrowband emissions that are trapped below the f_{ce} = 5 kHz surface. Such mode conversion is often induced by Z mode waves refracting near density irregularities or density gradients [*Oya and Morioka*, 1983]. The auroral zone is a likely source of the 5 kHz Z mode narrowband emissions, although there is still ambiguity in the exact location where these narrowband emissions are generated.

[30] **Acknowledgments.** The authors thanks J.-E. Wahlund and M. Morooka for providing the electron density measured by the RPWS Langmuir probe. The research reported in this paper was supported by NASA and the Cassini project through contract 1279973 from the Jet Propulsion Laboratory. S.Y. thanks Ann Persoon for helping with the illustrations.

[31] Philippa Browning thanks Ondrej Santolik and Stanley Cowley for their assistance in evaluating this paper.

References

Barbosa, D., W. S. Kurth, S. L. Moses, and F. L. Scarf (1990), Z mode radiation in Jupiter's magnetosphere: The source of Jovian continuum radiation, *J. Geophys. Res.*, *95*(A6), 8187–8196.

Cecconi, B., and P. Zarka (2005), Direction finding and antenna calibration through analytical inversion of radio measurements performed using a system of two or three electric dipole antennas on a three-axis stabilized spacecraft, *Radio Sci.*, *40*, RS3003, doi:10.1029/2004RS003070.

Cecconi, B., L. Lamy, P. Zarka, R. Prangé, W. S. Kurth, and P. Louarn (2009), Goniopolarimetric study of the Rev 29 perikrone using the Cassini/RPWS/HFR radio receiver, *J. Geophys. Res.*, *114*, A03215, doi:10.1029/2008JA013830.

Connerney, J. E. P., N. F. Ness, and M. H. Acuna (1982), Zonal harmonic model of Saturn's magnetic-field from Voyager-1 and Voyager-2 observations, *Nature*, *298*, 44–46.

Dougherty, M. K., et al. (2004), The Cassini magnetic field investigation, *Space Sci. Rev.*, *114*, 331–383.

Farrell, W. M., W. S. Kurth, M. L. Kaiser, M. D. Desch, D. A. Gurnett, and P. Canu (2005), Narrowband Z-mode emissions interior to Saturn's plasma torus, *J. Geophys. Res.*, *110*, A10204, doi:10.1029/2005JA011102.

Fischer, G., B. Cecconi, L. Lamy, S.-Y. Ye, U Taubenschuss, W. Macher, P. Zarka, W. S. Kurth, and D. A. Gurnett (2009), Elliptical polarization of Saturn Kilometric Radiation observed from high latitudes, *J. Geophys. Res.*, *114*, A08216, doi:10.1029/2009JA014176.

Gallagher, D., and D. Gurnett (1979), Auroral kilometric radiation: Time-averaged source location, *J. Geophys. Res.*, *84*, 6501–6509.

Galopeau, P. H. M., M. Y. Boudjada, and A. Lecacheux (2007), Spectral features of SKR observed by Cassini/RPWS: Frequency bandwidth, flux density and polarization, *J. Geophys. Res.*, *112*, A11213, doi:10.1029/2007JA012573.

Gurnett, D. A. (1975), The Earth as a radio source: The nonthermal continuum, *J. Geophys. Res.*, *80*, 2751–2763.

Gurnett, D. A., and A. Bhattacharjee (2005), *Introduction to Plasma Physics: With Space and Laboratory Applications*, pp. 124–125, Cambridge Univ. Press, Cambridge, U. K.

Gurnett, D. A., W. S. Kurth, and F. L. Scarf (1981), Narrowband electromagnetic emissions From Saturn's magnetosphere, *Nature*, *292*, 733–737.

Gurnett, D. A., S. D. Shawhan, and R. R. Shaw (1983), Auroral hiss, Z mode radiation, and auroral kilometric radiation in the polar magnetosphere: DE 1 observations, *J. Geophys. Res.*, *88*, 329–340.

Gurnett, D. A., W. Calvert, R. Huff, D. Jones, and M. Sugiura (1988), The polarization of escaping terrestrial continuum radiation, *J. Geophys. Res.*, *93*, 12,817–12,825.

Gurnett, D. A., et al. (2004), The Cassini radio and plasma wave investigation, *Space Sci. Rev.*, *114*, 395–463.

Gurnett, D. A., et al. (2005), Radio and plasma wave observations at Saturn from Cassini's approach and first orbit, *Science*, *307*, 1255–1259, doi:10.1126/science.1105356.

Hamaker, J. P., J. D. Bregman, and R. J. Sault (1996), Understanding radio polarimetry. I. Mathematical foundations. *Astron. Astrophys. Suppl. Ser.*, *117*, 137–147.

Hashimoto, K., and W. Calvert (1990), Observation of the Z mode with DE 1 and its analysis by three-dimensional ray tracing, *J. Geophys. Res.*, *95*, 3933–3942.

Jones, D. (1976), Source of terrestrial nonthermal radiation, *Nature*, *260*, 686–689.

Jones, D. (1980), Latitudinal beaming of planetary radio emissions, *Nature*, *288*, 225–229.

Kaiser, M. L., and M. D. Desch (1980), Narrow-band Jovian kilometric radiation: A new radio component, *Geophys. Res. Lett.*, *7*, 389–392.

Kaiser, M. L., M. D. Desch, W. M. Farrell, R. A. Hess, and R. J MacDowall (1993), Ordinary and Z-mode emissions from the Jovian Polar-region, *Planet. Space Sci.*, *41*, 977–985.

Kennel, C., R. Chen, S. Moses, W. Kurth, F. Coroniti, F. Scarf, and F. Chen (1987), Z mode radiation in Jupiter's magnetosphere, *J. Geophys. Res.*, *92*, 9978–9996.

Kraus, J. D. (1953), *Electromagnetics*, 407 pp., McGraw-Hill, New York.

Kraus, J. D. (1986), *Radio Astronomy*, 2nd ed., Cygnus-Quasar, Powell, Ohio.

Krimigis, S. M., et al. (2004), Magnetosphere imaging instrument (MIMI) on the Cassini mission to Saturn/Titan, *Space Sci. Rev.*, *114*, 233–329.

Lamy, L., P. Zarka, B. Cecconi, R. Prangé, W. S. Kurth, and D. A. Gurnett (2008), Saturn kilometric radiation: Average and statistical properties, *J. Geophys. Res.*, *113*, A07201, doi:10.1029/2007JA012900.

Lecacheux, A. (2000), Two antenna direction finding with purely circular polarization, paper presented at Cassini/RPWS team meeting presentation, Univ. of Iowa, Iowa City, Iowa.

Louarn, P., et al. (2007), Observation of similar radio signatures at Saturn and Jupiter: Implications for the magnetospheric dynamics, *Geophys. Res. Lett.*, *34*, L20113, doi:10.1029/2007GL030368.

Melrose, D. B. (1981), A theory for the nonthermal radio continua in the terrestrial and jovian magnetospheres, *J. Geophys. Res.*, *86*, 30–36.

Menietti, J. D., D. A. Gurnett, and J. B. Groene (2005), Radio emission observed by Galileo in the inner Jovian magnetosphere during orbit A-34, *Planet. Space Sci.*, *53*, 1234–1242.

Menietti, J. D., S.-Y. Ye, P. H. Yoon, O. Santolík, A. M. Rymer, D. A. Gurnett, and A. J. Coates (2009), Analysis of narrowband emission observed in the Saturn magnetosphere, *J. Geophys. Res.*, *114*, A06206, doi:10.1029/2008JA013982.

Oya, H., and A. Morioka (1983), Observational Evidence of Z and L-O Mode Waves as the Origin of Auroral Kilometric Radiation From the Jikiken (EXOS-B) Satellite, *J. Geophys. Res.*, *88*, 6189–6203.

Perraut, S., A. Roux, P. Louarn, D. Gurnett, W. Kurth, and K. Khurana (1998), Mode conversion at the Jovian plasma sheet boundary, *J. Geophys. Res.*, *103*, 14,995–15,000, doi:10.1029/97JA02879.

Persoon, A. M., D. A. Gurnett, W. S. Kurth, and J. B. Groene (2006), A simple scale height model of the electron density in Saturn's plasma disk, *Geophys. Res. Lett.*, *33*, L18106, doi:10.1029/2006GL027090.

Reiner, M., J. Fainberg, R. Stone, M. Kaiser, M. Desch, R. Manning, P. Zarka, and B.-M. Pedersen (1993), Source characteristics of Jovian narrow-band kilometric radio emissions, *J. Geophys. Res.*, *98*, 13,163–13,176, doi:10.1029/93JE00536.

Sonwalkar, V. S., et al. (2004), Diagnostics of magnetospheric electron density and irregularities at altitudes <5000 km using whistler and Z mode echoes from radio sounding on the IMAGE satellite, *J. Geophys. Res.*, *109*, A11212, doi:10.1029/2004JA010471.

Wang, Z., D. A. Gurnett, G. Fischer, S.-Y. Ye, W. S. Kurth, D. G. Mitchell, J. S. Leisner, and C. T. Russell (2010), Cassini observations of narrowband radio emissions in Saturn's magnetosphere, *J. Geophys. Res.*, *115*, A06213, doi:10.1029/2009JA014847.

Warwick, J. W., et al. (1979), Planetary radio astronomy observations from Voyager 2 near Jupiter, *Science*, *206*, 991–995.

Yoon, P., A. T. Weatherwax, and T. J. Rosenberg (1998), On the generation of auroral radio emissions at harmonics of the lower ionospheric electron cyclotron frequency: X, O and Z mode maser calculations, *J. Geophys. Res.*, *103*, 4071–4078, doi:10.1029/97JA03526.

Ye, S.-Y., et al. (2009), Source locations of narrowband radio emissions detected at Saturn, *J. Geophys. Res.*, *114*, A06219, doi:10.1029/2008JA013855.

B. Cecconi, Observatoire de Paris, F-92195 Meudon, France. (baptiste.cecconi@obspm.fr)

G. Fischer, Space Research Institute, Austrian Academy of Sciences, Schmiedlstrasse 6, Graz A-8042, Austria. (georg.fischer@oeaw.ac.at)

D. A. Gurnett, W. S. Kurth, J. D. Menietti, S.-Y. Ye, and Z. Wang, Department of Physics and Astronomy, University of Iowa, Iowa City, IA 52242, USA. (donald-gurnett@uiowa.edu; william-kurth@uiowa.edu; john-menietti@uiowa.edu; shengyi-ye@uiowa.edu; zhenzhen-wang@uiowa.edu)